Acta Cryst. (1969), A**25**, 143 E1·2

Experimental Absorption Correction: Results

BY R. HUBER AND G. KOPFMANN

Abteilung für Röntgenstrukturforschung am Max-Planck-Institut für Eiweiss- und Lederforschung, München und Physikalisch-Chemisches Institut der Technischen Hochschule München, Abteilung für Strukturforschung, München, Deutschland

The experimental determination of the transmission surface, which represents an approximation to the transmission of X-rays in crystals, is described. Experimental transmission surfaces are compared with values calculated from the crystal shape. Also structural parameters of some crystal structures obtained from data with and without experimental absorption correction are compared.

Introduction

In our first paper (Kopfmann & Huber, 1968) we showed that the transmission factor for X-rays through a crystal can be approximated by a product of two values of a three-dimensional function.

$$A_{p,s} = \frac{1}{V} \sum_i \exp -\mu[a_p(V_i)+a_s(V_i)]\Delta V_i \simeq A'_p \,.\, A'_s \,, \quad (1)$$

where

$$A'_p = \frac{1}{V} \sum_i \exp -\mu[a_p(V_i)]\Delta V_i \quad (2)$$

and

$$A'_s = \frac{1}{V} \sum_i \exp -\mu[a_s(V_i)]\Delta V_i \,.$$

($A_{p,s}$ is the transmission factor for a primary beam in direction **p** and secondary beam in direction **s**, μ is the linear absorption coefficient; $a_p(V_i)$ is the path length from the crystal surface to the volume element V_i for the primary beam; $a_s(V_i)$ is the path length from volume element V_i to the crystal surface for the secondary beam. A'_p and A'_s are the partial transmission factors for a primary beam in direction **p** and a secondary beam in direction **s** respectively.)

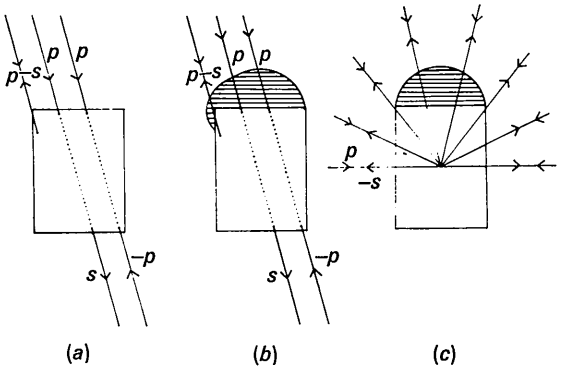

Fig. 1. Schematic diagram of sections through crystals with and without external absorber. The rays shown are individual rays of the primary (*p*) or secondary (*s*) beams. The arrows indicate the directions.

If the partial transmission A' is plotted from a mutual origin for all directions, one obtains a surface in three dimensions which we call the transmission surface. (The direction for a particular A' is the direction of the *absorption path*, *i.e.* the direction $-\mathbf{p}$ for a primary beam of direction **p** and the direction **s** for a secondary beam of direction **s**.)

In model calculations we were able to show that the approximation $A_{p,s} \simeq A'_p \,.\, A'_s$ is good for arbitrary and strongly anisometric crystal forms up to dimensions of 1 mm with a linear absorption coefficient of $\mu = 50\ \mathrm{cm}^{-1}$ (Kopfmann & Huber, 1968).

In order to determine the partial transmissions A' *experimentally* we measure the intensities of several reflexions in various rotational positions about their reciprocal lattice vectors **H**. The individual intensities vary due to the changes in absorption as the path lengths of the X-ray beams in the crystal vary. Each measurement provides an equation of the form

$$I^H_{p,s} = I^H \,.\, A'_p \,.\, A'_s \quad (3)$$

(where $I^H_{p,s}$ is the intensity measured for paths **p** and **s** and I^H is the corrected intensity.)

Taking logarithms we obtain a system of linear equations for the unknown partial transmissions A'.

Properties of the transmission surface

How is the partial transmission of a primary beam related to that of the secondary beam in the same direction? What relation is there if the directions are opposite?

Fig. 1(*a*) shows individual rays of a primary beam of direction **p** through a crystal. The individual volume elements irradiated by the rays are shown as dots. It is clear that for every volume element with a particular primary ray path length there is some volume element for which the primary ray in the opposite direction $-\mathbf{p}$ has the same path length. Thus when the contributions of all volume elements along all rays in the two beams are summed we obtain $A'_p = A'_{-p}$.

Similarly, the partial transmission for a primary beam of direction **p** is equal to that for a secondary

beam in the same direction $A'_p = A'_s$, and finally $A'_p = A'_{-s}$ the elementary paths in this case being completely identical. This means that the primary and secondary beams in the same or opposite directions have equal partial transmission. The transmission surface is therefore centrosymmetric. These relations are, however, only valid for Fig. 1(*a*) where the rays do not pass through an external absorber (mother liquor or glue).

Fig. 1(*b*) shows a crystal with an external absorber. It is clear from the diagram that here $A'_p \neq A'_{-p}$ and $A'_p \neq A'_s$ as only the primary beam in direction **p** has to traverse the external absorber. The relation $A'_p = A'_{-s}$, however, does remain valid. The transmission surface no longer has a centre of symmetry but nevertheless it describes the absorption properties also for a crystal with external absorber in a correct way.

Fig. 1(*c*) shows the directions for primary and secondary rays that occur when intensities are measured in one hemisphere only, using the symmetrical diffraction geometry (*cf.* section on methods of measurement). One can see that, regarding the definition of the directions of the partial transmissions A', only one hemisphere of the transmission surface has to be taken into account.

We therefore may deduce that reflexions measured in one hemisphere can be corrected using equations (3) and the transmission surface determined for this hemisphere. The partial transmissions then yield the true transmission factor [according to the approximation (1)] for any crystal shape with external absorber.

Determination of the transmission surface

As shown in model calculations the curvature of the transmission surface is fairly uniform even if the crystal shape is far from spherical and the absorption coefficient large. We may, therefore, define the transmission surface with uniformly distributed lattice points, and the partial transmission for directions between the lattice points may be determined by interpolation.

As mentioned above, the observations made to determine the transmission surface yield equations of the form

$$\log I^H_{p,s} = \log I^H + \log A'_p + \log A'_s \,. \qquad (4)$$

Log A'_p (and log A'_s) can be described as a linear combination of the neighbouring lattice points of the transmission surface:

$$\log A'_p = n \sum_i a_i \log A'_i \,, \qquad (5)$$

where A'_i are the partial transmissions at the neighbouring lattice points, a_i is inversely proportional to the angular distance from $-\mathbf{p}^*$ to lattice point i and n is a normalization factor. The actual unknowns are the A'_i, the values of the transmission surface at the lattice points.

* The direction of A_p' is, as mentioned, defined as $-\mathbf{p}$.

In the system of linear equations (4) the I^H are also unknowns and have to be determined as well. They are by no means worthless side products and can be used indirectly to determine the absorption corrections for the individual reflexions (Kopfmann & Huber, 1968). They can also be used to scale the reflexions of different crystals of the same substance as they are values of high precision, having been measured several times. This is of importance for protein crystal structure analysis.

In the course of our determinations of transmission surfaces for a large number of crystals it has occurred that the values at the lattice points were poorly deter-

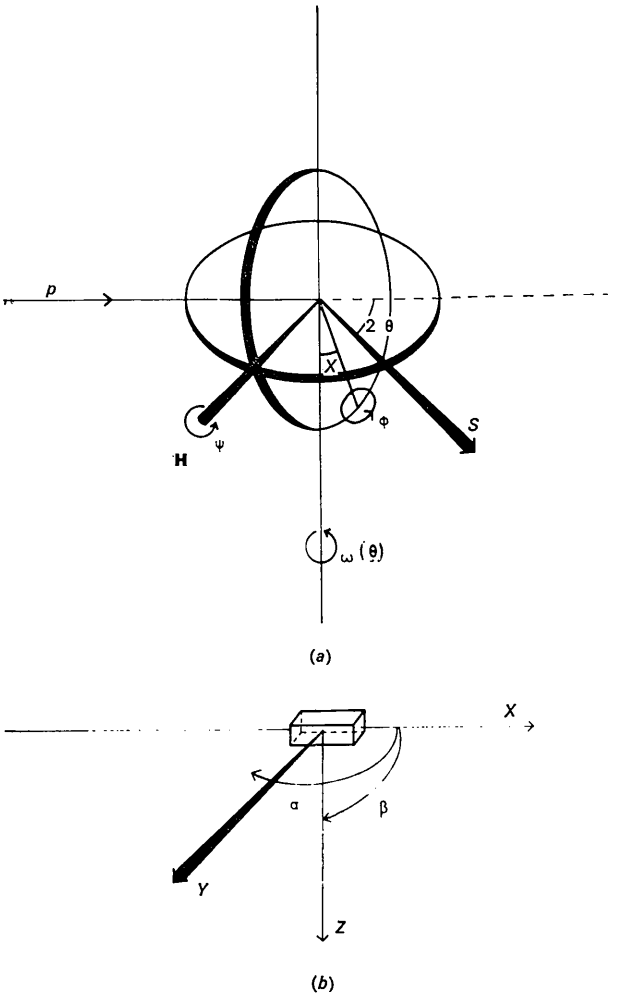

Fig. 2. (*a*) Schematic diagram of a 4-circle diffractometer. *p* and *s* are the primary and secondary beams, **H** is the reciprocal lattice vector of a set of planes in the reflecting position. The four circles of the diffractometer are the 2θ, ω, χ and φ circles. ψ is the rotation angle about **H** and is called the azimuth. (*b*) The set of cartesian axes used to describe the crystal. When all the diffractometer circles are set to zero *p* coincides with *x* and the ω axis with *z*. *y* is then chosen perpendicular to *x* and *z* to form a right-handed set. The definition of the polar angles α and β is clear from the Figure.

mined, *i.e.* they did not form a smooth surface. This was due either to the number of measurements being too small or too inaccurate in their measurement. The following methods of improving the surface have been used:

(*a*) Elimination of obviously bad observations.

(*b*) Shifting the values at individual lattice points that were far from the surface formed by the other values onto this surface.

(*c*) Application of the procedure described by Kopfmann & Huber (1968) for smoothing the transmission surface using the I^H.

(*d*) Describing the transmission surface as a function of the 4th power.

Methods of measurement

The basis for the determination of the partial transmission A' is the measurement of individual reflexions of various rotational positions about their reciprocal lattice vectors **H**. This rotation can be produced by suitable rotation of the ω, χ and φ circles of a 4-circle goniometer.

Fig. 2(*a*) shows the geometry of a 4-circle diffractometer. The designation of the circles is the conventional one. The cartesian system used to describe the crystal is shown in Fig. 2(*b*).

The mathematical formulation of the rotation of a crystal about a reciprocal lattice vector and the calculation of the corresponding diffractometer angles ω, χ and φ will not be repeated here. This can be found elsewere *e.g.* in the paper by Busing & Levy (1967). The calculation of the directions of the primary and secondary beams relative to the crystal coordinate system at given diffractometer settings can also be obtained from this article. The formulae that we use differ from those given by Busing & Levy as the crystal coordinate system in which we work is rotated.

As mentioned above, the transmission surface should be determined using measurements in one hemisphere and applied to correct reflexions measured in the same hemisphere. This means that normally the transmission surface need only be determined in the range $\beta = 0$–$90°$ and $\alpha = 0$–$360°$. If the maximum diffraction angle (2θ) for reflexions that have to be corrected is less than 180°, $\beta_{max} < 90$. If the diffraction geometry is symmetrical with the χ circle of the diffractometer bisecting the angle between **p** and **s** (this is the usual set-up) then $\beta_{max} = \theta_{max}$. This is only strictly true for reflexions measured at $\chi = 90°$. For $\chi < 90°$: $\beta < \theta$.

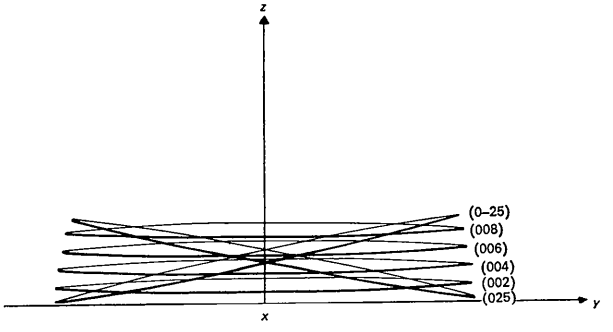

Fig. 3. The primary and secondary beam directions that occur when the 002, 004, 006, 008, 025 and $0\bar{2}5$ reflexions of TCPRC are rotated.

Experimental results

Choice of reflexions

Our measurements are made on a Siemens AED diffractometer. Its design with an open Eulerian cradle limits χ to a maximum value of 90°. The diffractometer has three setting motors for the angles ω, χ and φ. The detector is driven by the ω motor with a 2:1 gear ratio but can be disconnected. This means that reflexions can be measured in various settings of the azimuthal angle with a 'moving crystal-fixed counter' procedure. Which reflexions should we choose for the determination of the transmission surface using equations (3)?

(*a*) The reflexions should be strong in order to keep the counting time low and the accuracy high, but reflexions should be avoided that are weakened by extinction.

(*b*) It should be possible to rotate the reflexions through a large azimuthal angle so that many equations (3) can be obtained from one reflexion. On our diffractometer, reflexions at $\chi = 90°$ (axial reflexions) can be rotated through a full 360° and those off the axes through a smaller angle.

(*c*) It is also advantageous to use equivalent reflexions as further equations can thus be obtained without having to introduce a new and unknown I^H. Fig. 3 shows the region of the transmission surface that is covered by rotating the reflexions 002, 004, 006, 008, 025 and $0\bar{2}5$ of TCPRC.* The paths of the 025 and $0\bar{2}5$ reflexions have also been drawn as full circles but only about $\frac{1}{3}$ of the full azimuthal circle could in fact be traced owing to the restriction in the movement of the diffractometer circles. (It should be mentioned that these reflexions alone do not suffice for a calculation of the transmission surface.)

(*d*) The number of individual measurements required for a determination of the transmission surface depends on the number of unknowns *i.e.* on the number of lattice points of the surface. We consider an angular distance between points of 12–15° to be sufficient. This means about 100–150 unknowns for the full hemisphere of the transmission surface. In most cases, however, only a part of the surface has to be determined. We usually make 500–800 individual measurements (for proteins only about 300 owing to the limited resolution). This ensures that the system of equations is overdetermined to a sufficient extent.

* Tris(cyclopentodienylrhodium carbonyl)

Measurements

All intensity measurements for the determination of the transmission surface were made using the 'moving crystal-fixed counter' procedure. The background was measured on both sides of the reflexion and subtracted. Fig. 4 shows the integrated intensities of the axial reflexions of TCPRC plotted against the azimuthal angle. For the 002 reflexion, spikes occur in the intensity curve that lie well outside the error of the measurement. These can be explained as being due to double reflexion.

Fig. 5 shows intensity-azimuth curves of several near-axial reflexions of fusicoccin. (Crystal dimensions roughly $0{\cdot}6 \times 0{\cdot}3 \times 0{\cdot}6$ mm; 0·6 mm in the direction of the φ axis, Cu $K\alpha$ radiation, $\mu = 9$ cm^{-1}.) The azimuthal rotation obtainable with the diffractometer varies in range. One notices that the slope of the curve changes fairly continuously in going from the $4\bar{2}6$ to the $5\bar{2}6$ reflexion. A large fraction of the transmission surface is mapped by these reflexions.

Comparison of measured and calculated transmission surfaces

We have made a comparison of the measured transmission surface and the one calculated using equation (2) for a number of low-molecular organic crystals. All the crystals were fragments held in Lindemann tubes with grease. The measurement of the crystal shape under these conditions is rather difficult and always inaccurate. We had to assume more-or-less idealized crystal shapes. We believe that the fact that the capillary and the grease could not be taken into account is the main reason for the systematic differences that arose in some cases between the calculated and measured transmission surfaces, as the differences only arose when Cu radiation was used and not for Mo radiation.

A further cause of an (apparent) systematic difference can lie in the scaling of measured and calculated transmission surfaces. We scaled by setting measured and calculated partial transmission equal to one another for a particular direction.

(*a*) TCPRC [tris(cyclopentadienylrhodium carbonyl)]* (Paulus, 1968): The crystal dimensions were 0·09 $\times 0{\cdot}23 \times 0{\cdot}55$ mm. The 0·55 mm axis is the φ or Z axis of the crystal. (These dimensions do not describe the crystal shape actually used in the calculation but are merely intended to give an indication of the overall crystal size. The same holds for all other crystals discussed.) The linear absorption coefficient for Mo $K\alpha$

* In collaboration with Dr E. Paulus.

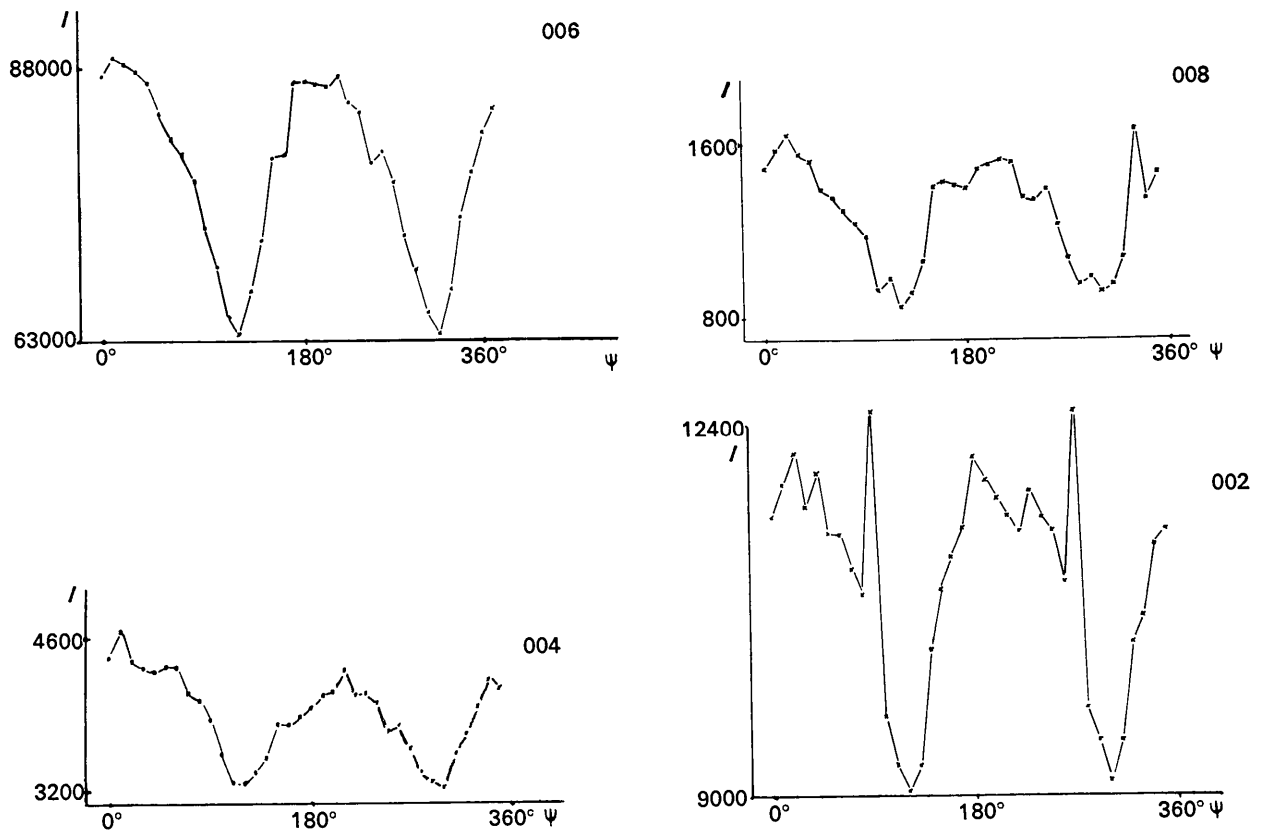

Fig. 4. Intensity curves of the axial reflexions of TCPRC plotted against azimuthal angle.

radiation was 20 cm^{-1}. The agreement between measured and calculated transmission surface is good (Fig. 6).

(*b*) γ-Rhodomycinone* (Amit, Brandl, Brodherr, Gieren, Hädicke, Hoppe, Huber & Röhrl, 1967): The crystal dimensions were 0·08 × 0·64 × 0·60 mm (0·60 in the **Z** direction) $\mu_{Cu\ K\alpha} = 7{\cdot}6\ cm^{-1}$. The short axis of the measured transmission surface is smaller than that of the calculated surface for all sections (Fig. 7). This behaviour indicates that the crystal shape was probably measured inaccurately. If the dimensions of the platelet (0·08 × 0·64 mm) differed even more, then the eccentricity of the elliptical transmission sections would also be greater.

(*c*) *N*-Bromo-acetyl-D-ala-L-ala-*p*-bromo-anilide† (Lotter, 1968): The crystal dimensions were 0·07 × 0·16 × 0·34 mm (0·34 in the **Z** direction) $\mu_{Cu\ K\alpha} = 95{\cdot}5\ cm^{-1}$. The systematic difference between the calculated and measured transmission surface in the 0° and 48° sections (Fig. 8) could be explained as being due to the grease, as its absorption effect decreases as the angle β increases.

(*d*) Azepin-iron-tricarbonyl* (Amit, Brandl, Brodherr, Gieren, Hädicke, Hoppe, Huber & Röhrl, 1967): The crystal dimensions were 0·3, 0·2 and 0·45 mm (0·45 in the **Z** direction) $\mu_{Mo\ K\alpha} = 18\ cm^{-1}$. The measured and calculated transmission surfaces agree well (Fig. 9).

(*e*) Iodo-resistomycin†: The crystal dimensions were 0·14 × 0·04 × 0·42 mm (0·42 in the **Z** direction) $\mu_{Cu\ K\alpha} = 123\ cm^{-1}$. Apart from the fact that the scale factor chosen was somewhat small, there are no systematic differences to be seen in Fig. 10. The marked plate-like shape of the crystal is reflected in conspicuous cusps in the transmission sections in the direction of their short axes. (The reason for the marked deviation of some points from a smooth curve lies in the fact that only 170 measurements were used for the determination of the transmission surface.)

* In collaboration with Mr M. Röhrl.
† In collaboration with Mr H. Lotter.

* In collaboration with Mr A. Gieren.
† In collaboration with Dr F. Brandl.

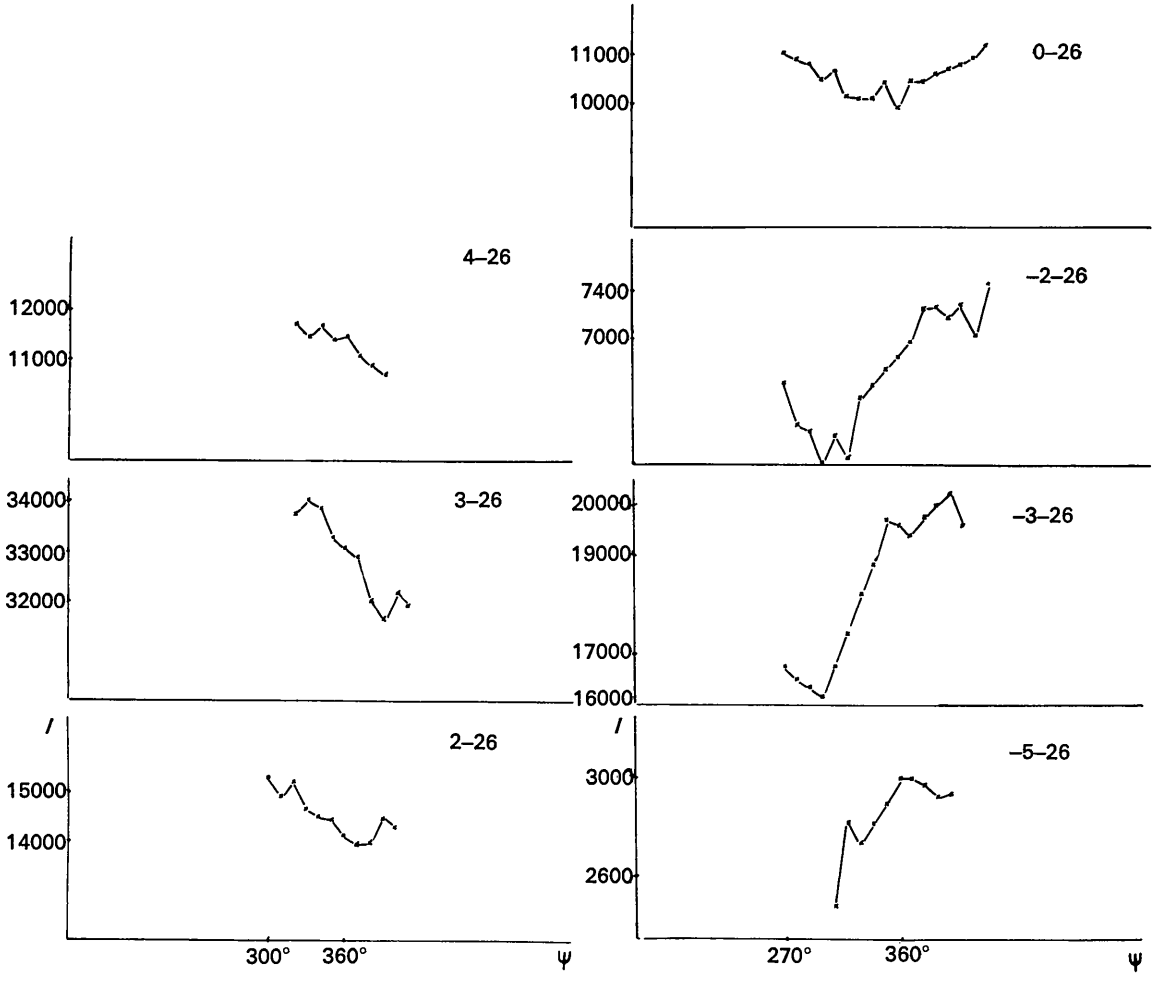

Fig. 5. Intensity – azimuth curves of a number of near-axial reflexions for fusicoccin.

Comparison of structure parameters obtained by refining data with and without the empirical absorption correction

Three structures were investigated, the refinements being made to completion. The results can be summarized as follows:

(i) The R factor could be improved by between 1 and 2% depending on the size of the absorption correction *i.e.* on the crystal size and shape.

(ii) The changes in the temperature factors and surprisingly enough also in the bond lengths produced by application of the absorption corrections are considerable, although the R factors have in some cases been refined to about 6% without absorption correction.

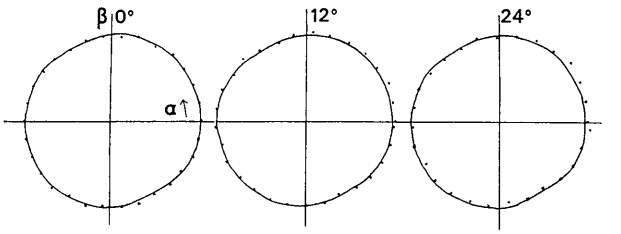

Fig. 6. Measured (×) and calculated (−) sections of the transmission surface for TCPRC. (*In this and the following figures the transmission surface for the structure amplitudes (i.e. $\sqrt{A'}$) is drawn.*)

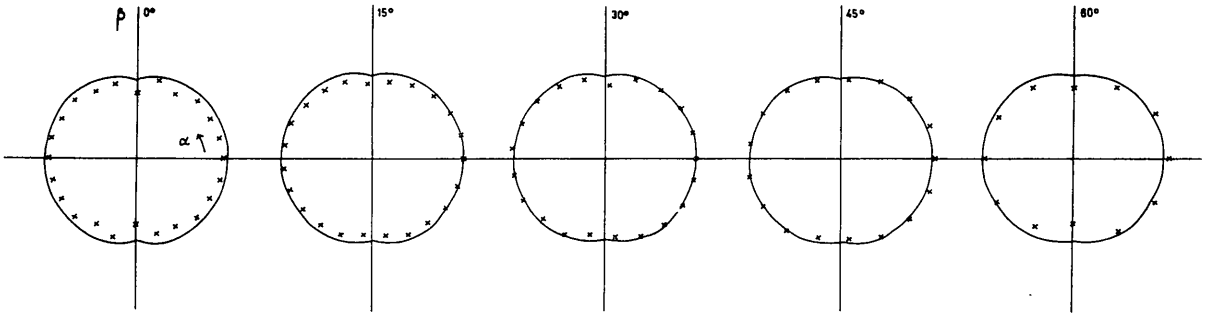

Fig. 7. Measured (×) and calculated (−) transmission surface for γ-rhodomycinone.

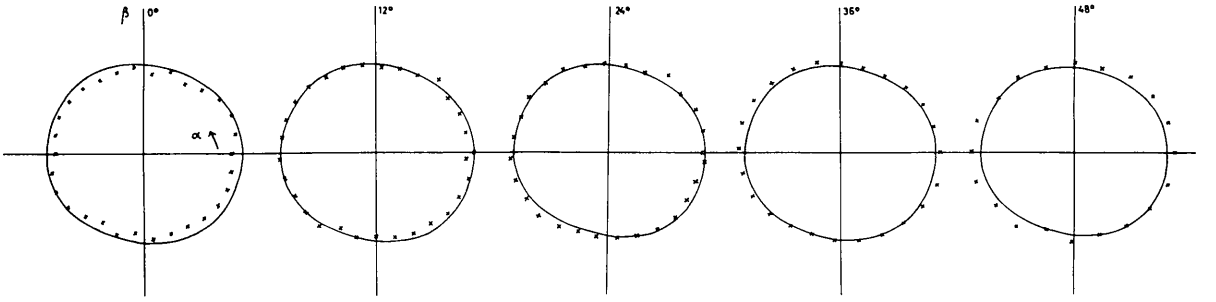

Fig. 8. Measured (×) and calculated (−) transmission surface for *N*-bromo-acetyl-D-ala-L-ala-*p*-bromo-anilide.

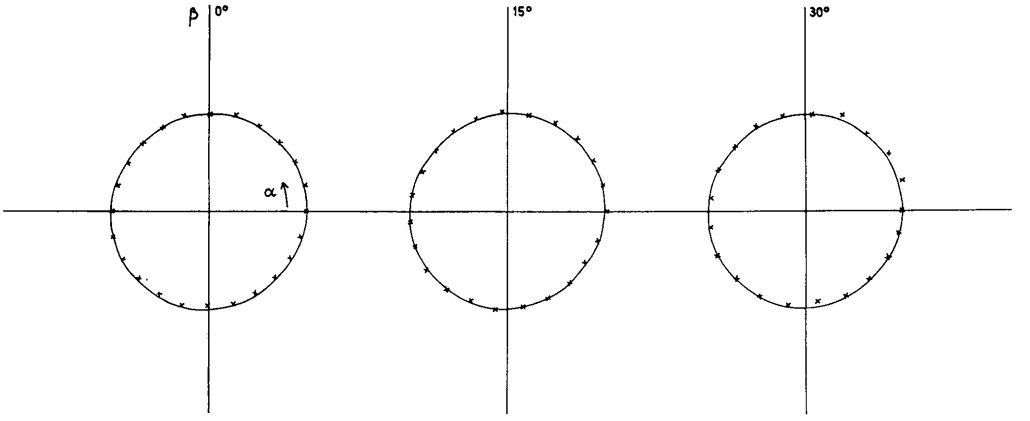

Fig. 9. Measured (×) and calculated (−) transmission surface for azepin-iron-tricarbonyl.

(iii) The changes in bond lengths are in some cases as high as 5σ in magnitude (σ is the standard deviation of the bond length).

(iv) The absorption correction improves the bond lengths considerably.

(v) Difference Fourier syntheses made with corrected data are much clearer and the hydrogen atoms can be found in these much more easily.

(*a*) γ-Rhodomycinone:

The transmission surface of this crystal was shown in Fig. 7. The structure contains two molecules in the asymmetric unit, which permits a comparison of equivalent bonds before and after absorption correction (Table 1). The experimentally determined partial transmissions were used directly for the correction. It can be seen that the four largest differences (of up to 0·05 Å) are reduced to 0·03 or 0·02 Å by the absorption correction (σ before absorption correction was ~0·01 Å). Also the consistency of bond lengths within one molecule increased considerably [C(3)–C(5) compared with C(10)–C(7), C(3)–C(6) with C(6)–C(10), C(5)–O(5) with C(7)–O(3)]. The *R*-factor dropped from 6·8% to 4·8%. Fig. 11 shows the hydrogen atoms before ab-

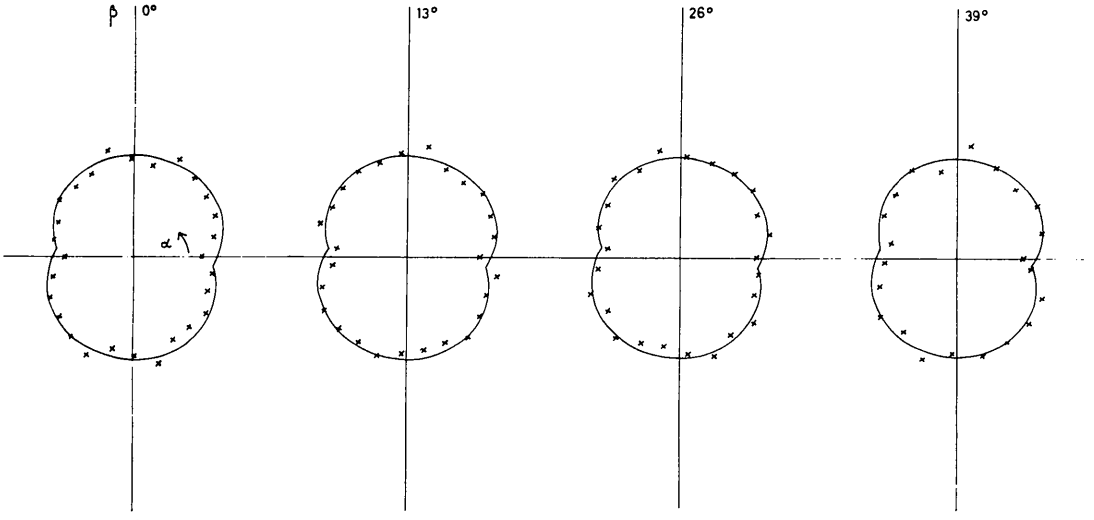

Fig. 10. Measured (×) and calculated (−) transmission surface of iodo-resistomycin.

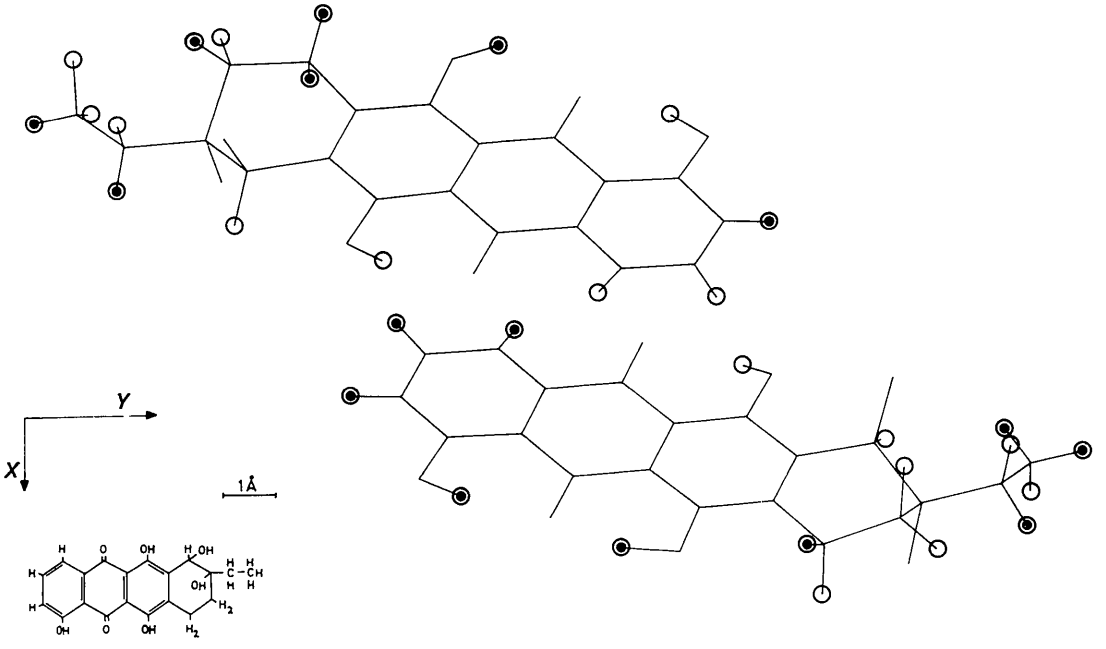

Fig. 11. Hydrogen atoms found before absorption correction ⊙ and those which additionally became visible after correction ○.

sorption correction ⊙ and those which became additionally visible after correction o. Almost all hydrogen atoms could be identified after absorption correction.

(*b*) *N*-Bromo-acetyl-D-ala-L-ala-*p*-bromo-anilide:

The transmission surface of this crystal was shown in Fig. 8. The correction was made using a function of the 4th power obtained from the experimental partial transmissions. The *R*-factor improved from 6·7 to 5·5%. Table 2 compares the bond lengths in the molecule after refinement with and without absorption correction. The value of σ calculated for bonds between light atoms was 0·014 Å. Thus changes as large as 4–5σ occured. It can be seen that the bond lengths in the benzene ring become far more realistic after absorption correction. The C=O carboxyl bond length also changes markedly. The value of 1·24 Å after correction is the normally accepted value (1·18 Å before correction).

(*c*) Azepin-iron-tricarbonyl:

The measured transmission surface is shown in Fig. 9. The correction was done using the experimental partial transmission directly. The *R*-factor improved from 6·7 to 6·3%. As the transmission surface is virtually spherical the effect of the absorption correction on the bond lengths is small. One finds, however, large changes in the temperature factors of the hydrogen atoms, which have also been refined. These parameters are undoubtedly the most sensitive parameters to absorption errors. Table 3 shows the isotropic temperature factors before and after absorption correction. The temperature factors after correction are much more realistic and consistant.

Table 1. *Equivalent bond lengths of γ-rhodomycinone*

	Before absorption correction		After absorption correction	
	Molecule 1	Molecule 2	Molecule 1	Molecule 2
C(5)—C(1)	1·43	1·38	1·42	1·39 !
C(1)—C(11)	1·40	1·39	1·37	1·37
C(11)–C(9)	1·39	1·38	1·39	1·40
C(9)—C(13)	1·38	1·39	1·38	1·37
C(13)–C(3)	1·44	1·42	1·42	1·42
C(13)–C(4)	1·47	1·47	1·48	1·48
C(4)—O(1)	1·26	1·26	1·25	1·25
C(4)—C(14)	1·45	1·46	1·44	1·46
C(14)–C(10)	1·44	1·45	1·43	1·43
C(14)–C(2)	1·38	1·37	1·39	1·39
C(2)—O(4)	1·36	1·35	1·35	1·34
C(2)—C(12)	1·42	1·43	1·41	1·43
C(12)–C(8)	1·40	1·40	1·38	1·39
C(12)–C(15)	1·53	1·48	1·54	1·51 !
C(15)–O(6)	1·45	1·45	1·44	1·44
C(15)–C(17)	1·53	1·56	1·53	1·54 !
C(17)–O(7)	1·47	1·44	1·45	1·43
C(17)–C(19)	1·52	1·54	1·53	1·54
C(19)–C(20)	1·53	1·54	1·52	1·51
C(17)–C(18)	1·54	1·53	1·53	1·51
C(18)–C(16)	1·51	1·52	1·52	1·52
C(16)–C(8)	1·50	1·50	1·51	1·51
C(8)—C(7)	1·40	1·41	1·41	1·42
C(7)—O(3)	1·35	1·35	1·35	1·35
C(7)—C(10)	1·42	1·38	1·41	1·39 !
C(10)–C(6)	1·42	1·44	1·44	1·45
C(6)—O(2)	1·27	1·26	1·26	1·26
C(6)—C(3)	1·47	1·46	1·47	1·46
C(3)—C(5)	1·37	1·39	1·40	1·41
C(5)—O(5)	1·37	1·36	1·35	1·34

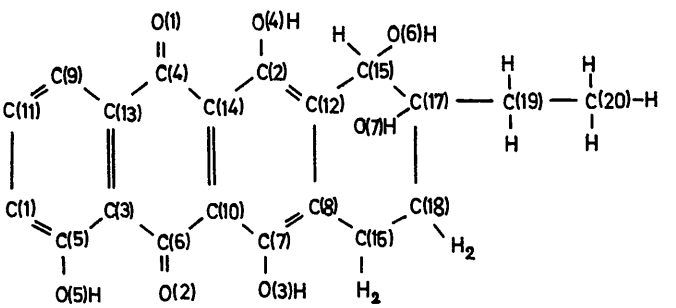

Table 2. *Comparison of bond lengths in N-bromo-acetyl-*D*-ala-*L*-ala-p-bromo-anilide*

	Before absorption correction	After absorption correction
Br(1)–C(1)	1·94	1·93
Br(2)–C(14)	1·93	1·93
C(1)—C(2)	1·44	1·38 !
C(2)—C(3)	1·45	1·43 !
C(3)—C(4)	1·41	1·41
C(4)—C(5)	1·39	1·40
C(5)—C(6)	1·41	1·41
C(6)—C(1)	1·36	1·41 !
C(4)—N(1)	1·48	1·46
N(1) –C(7)	1·37	1·37
C(7)—O(1)	1·22	1·22
C(7)—C(8)	1·54	1·52
C(8)—C(9)	1·48	1·50
C(8)—N(2)	1·48	1·47
N(2) –C(10)	1·37	1·37
C(10)–O(2)	1·18	1·24 !
C(10)–C(11)	1·56	1·53
C(11)–C(12)	1·57	1·56
C(11)–N(3)	1·46	1·47
N(3) –C(13)	1·35	1·36
C(13)–C(14)	1·53	1·52
C(13)–O(3)	1·23	1·24

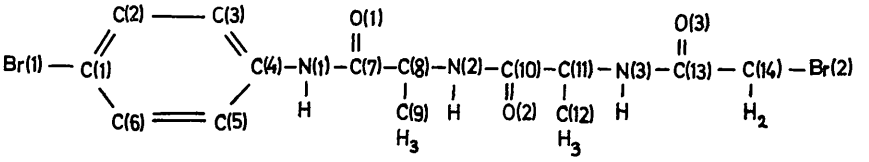

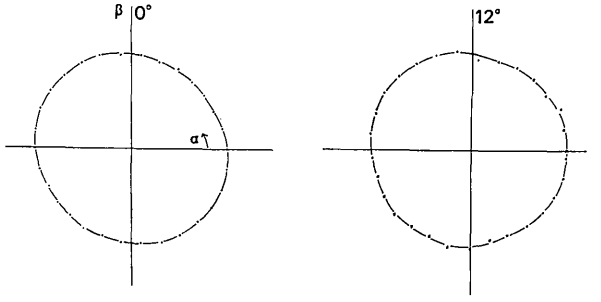

Fig. 12. Transmission surface (×) of erythrocruorin nat. Crystal No. 156.

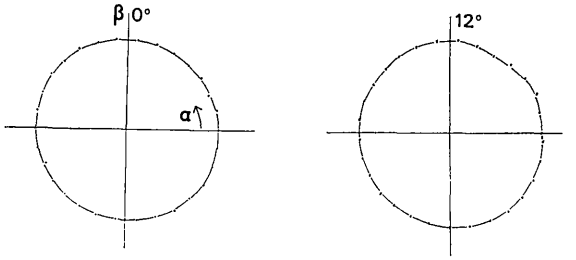

Fig. 13. Transmission surface (×) of erythrocruorin SeCN derivative. Crystal No. 149.

Table 3. *Comparison of hydrogen atom temperature factors* (Å^2) *in azepin-iron-tricarbonyl*

Before absorption correction	After absorption correction
7·6	7·0
12·3	7·1
10·1	8·1
4·8	4·3
5·3	4·7
7·2	6·9
7·7	6·1
2·2	2·3
5·5	5·7
5·0	4·5
6·2	6·2
4·6	5·2
3·4	2·7
12·9	10·6

Comparison of equivalent reflexions in proteins before and after absorption correction

The experimental absorption correction is of particular significance for protein crystals as (*a*) it is impossible to determine the shape of the crystal with much accuracy when it is covered with buffer solution, (*b*) the absorption coefficient of the buffer solution is in general of the same order of magnitude as that of the crystal itself and therefore has to be taken into account and (*c*) the accuracy of the measurement required is usually greater than for other substances. Figs. 12 and 13 show transmission surfaces of erythrocruorin

crystals (Huber, Formanek & Epp, 1968). The angle β to which the transmission surface has to be measured is small as these crystals were only measured to a value of $\theta = 13°$.

The comparison of equivalent reflexions of the erythrocruorin crystals used before and after absorption correction is a very good indication of how effective the correction is. As the symmetry of the crystal is trigonal the equivalent reflexions occur at quite different χ and φ angles. The correction was performed using the partial transmission factors (Figs. 12 and 13) directly. About 150 pairs of reflexions were measured in each case and the statistical correlation calculated before and after correction ($R = \Sigma |\Delta F| / \Sigma |F|$ where ΔF is the difference in structure amplitude of two equivalent reflexions).

	Crystal number	R in %: Before correction	R in %: After correction
Er nat	156	8·1	3·8
Er SeCN derivative	149	6·3	3·8
Er $Pt(NO_2)_2(NH_3)_2$ derivative	182	2·3	2·0
Er $Hg(az)_2$ derivative	201	6·6	2·6

We wish to thank Professor W. Hoppe for many helpful discussions and also Dr F. Brandl, Mr A. Gieren, Mr H. Lotter, Dr E. Paulus and Mr M. Röhrl for making diffractometer measurements and for help with the evaluation.

This publication has been supported by the Deutsche Forschungsgemeinschaft, the Fonds der Chemischen Industrie and the Badische Anilin- & Soda-Fabrik. We should like to express our sincere thanks.

References

Amit, A., Brandl, F., Brodherr, N., Gieren, A., Hädicke, E., Hoppe, W., Huber, R. & Röhrl, A. (1967). Sektion für Kristallkunde der Deutschen Mineralogischen Gesellschaft, 9. Diskussionstagung, Bonn und Jülich, Referate, 53.

Busing, W. R. & Levy, H. A. (1967). *Acta Cryst.* **22**, 458.

Huber, R., Formanek, H. & Epp, O. (1968). *Naturwissenschaften*, **55**, 75.

Kopfmann, G. & Huber, R. (1968). *Acta Cryst.* A**24**, 347.

Lotter, H. (1968). Dissertation, Technische Hochschule, München.

Paulus, E. F. (1968). *Acta Cryst.* In the press.

DISCUSSION

Milledge: Why are the bond lengths so different? Surely absorption affects principally the low-angle reflexions. A proper weighting scheme should ensure that the bond lengths are not so much affected by those.

Huber: Absorption also affects the high-angle reflexions strongly.

A Questioner: How did absorption affect the temperature factors?

Huber: More than the bond lengths, but with anisotropic temperature factors it is difficult to judge an improvement objectively.

Coppens: The experimental determination of the transmission surface is very sensitive to anisotropic extinction.

Huber: We omit very strong reflexions.

Coppens: I would not expect your approximations to be very good for highly absorbing crystals.

Huber: Model calculations show that the approximation is good if $\mu d < 3$ or 4 (μ, linear absorption coefficient; d, dimension).

Furnas: Is it not better to measure the geometrical shape of the crystal before it is mounted and to compute the absorption? (*cf.* de Meulenaer, J. & Tompa, H. (1965), *Acta Cryst.* **19**, 1014; Coppens, P., de Meulenaer, J. & Tompa, H. (1967), *Acta Cryst.* **22**, 601).

Huber: You must know the exact orientation of the crystal in the actual experiment in order to make valid corrections. In addition, in protein crystallography we want to know the absorption of drops of mother liquor.